Non-invasively measured brain activity and radiological progression in diffuse glioma

T. Numan[1,2], S.D. Kulik[1,2], B. Moraal[3], J.C. Reijneveld[2,4], CJ. Stam[5], P.C. de Witt Hamer[2,6], J. Derks[1,2], A.M.E. Bruynzeel[7], M.E. van Linde[2,4], P. Wesseling[2,8], M.C.M. Kouwenhoven[2,4], M. Klein[2,9], T. Würdinger[6], F. Barkhof[3,10], J.J.G. Geurts[1], A. Hillebrand[5], L. Douw[1,2*]

[1] Department of Anatomy and Neurosciences, Amsterdam UMC, Vrije Universiteit Amsterdam, The Netherlands

[2] Brain Tumor Center Amsterdam, Amsterdam UMC, Vrije Universiteit Amsterdam, The Netherlands

[3] Department of Radiology and Nuclear Medicine, Amsterdam UMC, Vrije Universiteit Amsterdam, Amsterdam, The Netherlands

[4] Department of Neurology, Amsterdam UMC, Vrije Universiteit Amsterdam, The Netherlands

[5] Department of Clinical Neurophysiology and MEG Center, Amsterdam UMC, Vrije Universiteit Amsterdam, The Netherlands

[6] Department of Neurosurgery, Amsterdam UMC, Vrije Universiteit Amsterdam, The Netherlands

[7] Department of Radiotherapy, Amsterdam UMC, Vrije Universiteit Amsterdam, The Netherlands

[8] Department of Pathology, Amsterdam UMC, Vrije Universiteit Amsterdam, The Netherlands

[9] Department of Medical Psychology, Amsterdam UMC, Vrije Universiteit Amsterdam, The Netherlands

[10] Department of Radiology, Institutes of Neurology & Helathcare Engineering, University College London, United Kingdom

Abstract

Non-invasively measured brain activity is related to progression-free survival in glioma patients, suggesting its potential as a marker of glioma progression. We therefore assessed the relationship between brain activity and increasing tumor volumes on routine clinical magnetic resonance imaging (MRI) in glioma patients. Postoperative magnetoencephalography (MEG) was recorded in 45 diffuse glioma patients. Brain activity was estimated using three measures (absolute broadband power, offset and slope) calculated at three spatial levels: global average, averaged across the peritumoral areas, and averaged across the homologues of these peritumoral areas in the contralateral hemisphere. Tumors were segmented on MRI. Changes in tumor volume between the two scans surrounding the MEG were calculated and correlated with brain activity. Brain activity was compared between patient groups classified into having increasing or stable tumor volume. Results show that brain activity was significantly increased in the tumor hemisphere in general, and in peritumoral regions specifically. However, none of the measures and spatial levels of brain activity correlated with changes in tumor volume, nor did they differ between patients with increasing versus stable tumor volumes. Longitudinal studies in more homogeneous subgroups of glioma patients are necessary to further explore the clinical potential of non-invasively measured brain activity.

Introduction

Monitoring treatment response and disease progression in diffuse glioma patients is challenging. The current standard for monitoring tumor growth is magnetic resonance imaging (MRI), namely T1-weighted scans before and after contrast injection, a T2-weighted scan and a fluid-attenuated inversion recovery (FLAIR) sequence[1]. However, determining growth can be challenging[2]. Moreover, other patient factors such as cognitive deterioration may precede radiological progression[3,4], underlining the relevance of exploring alternative markers of growth.

There is a causal relationship between increased peritumoral neuronal activity (i.e. spiking rate) and accelerated glioma growth[5,6]. Moreover, glutamate-dependent 'neurogliomal' synapses are formed between healthy neurons and nearby glioma cells, resulting in interconnected glioma and neuronal networks[7,8]. Based on these studies, it seems that both higher spiking rates and greater glutamate-related excitation cause increased proliferation and invasion of glioma, at least in animal models. Translating these findings to patients, glioma-infiltrated brain regions showed greater neuronal activity measured with intraoperative electrocorticography as compared to healthy appearing regions in three glioblastoma (GBM) patients[8], further supporting this association between brain and tumor activities.

In recent translational studies, magnetoencephalography (MEG) was established as a non-invasively measured proxy of neuronal activity[9]. MEG records the magnetic fields induced by (mainly) postsynaptic neuronal currents with high temporal and varying spatial resolution[10,11]. Each sensor's time-series reflects brain activity across different frequencies. The power spectrum can be determined to reduce these multidimensional data to a single indication of brain activity. This spectrum reflects the squared amplitude of all frequencies (figure 1), and the broadband power is the sum of squared amplitudes across all frequencies. We previously found that higher global broadband power at diagnosis and after tumor resection relates to shorter progression-free survival (PFS[12,13]), also after taking known predictors into account, and may thus be an early marker of tumor progression. As a next step in the investigation of the clinical relevance of non-invasively measured brain activity, we aimed to relate brain activity to ongoing radiological glioma growth.

Figure 1. Schematic analysis pipeline of brain activity and tumor volumes

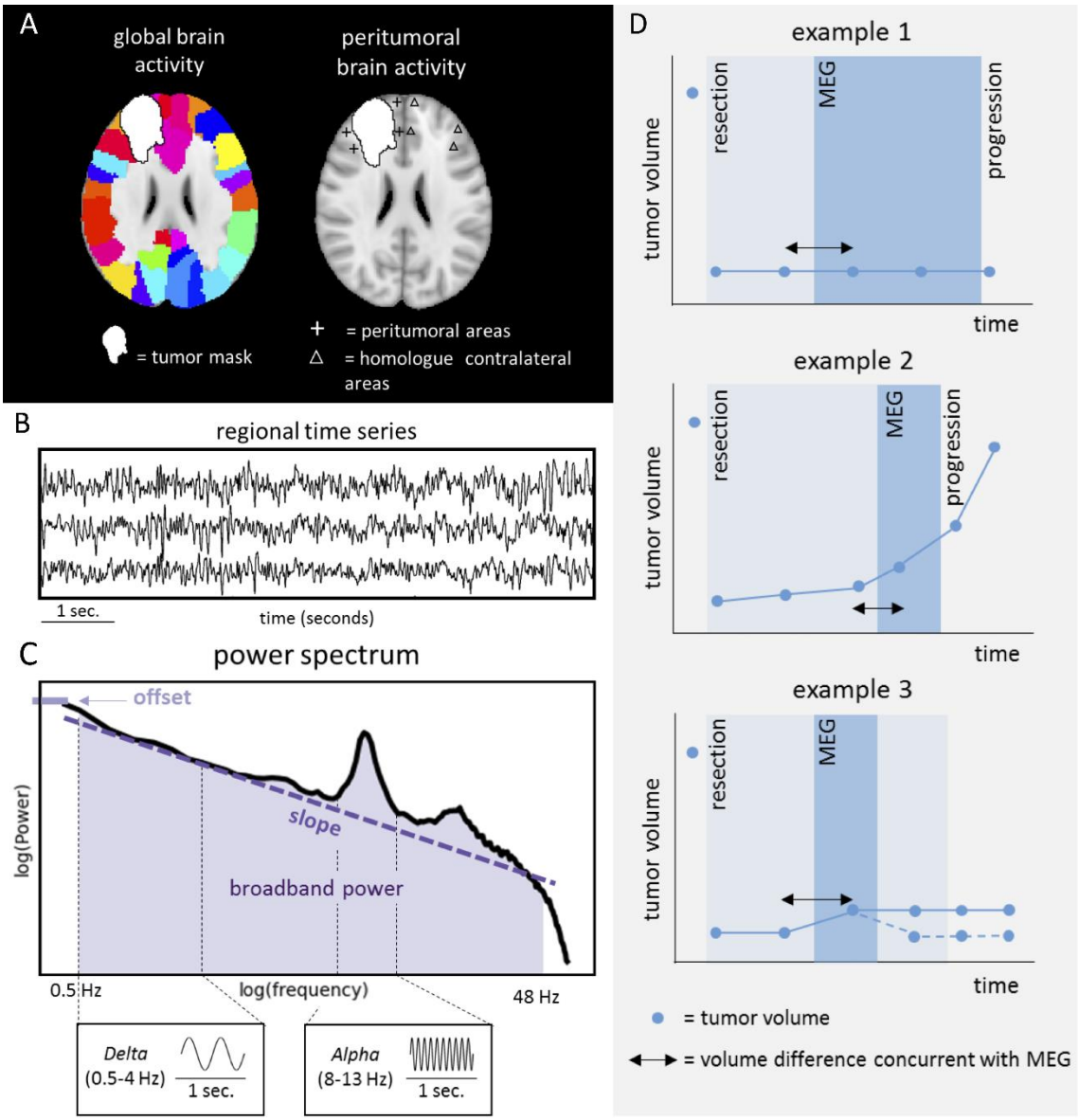

***Legend**. A) Time-series were extracted across regions (left panel) and then averaged to obtain estimates of global brain activity. Peritumoral brain activity was obtained using peritumoral areas (cross hairs) at maximum 3 cm of the tumor or resection cavity and thereafter normalized according to activity of homologue contralateral regions (triangles). B) Three exemplar regional time-series. C) The power spectrum shows which frequencies, and with which strength, are present in the time-series, with slower frequencies on the left (e.g. delta 0.5-4Hz) and faster frequencies on the right (e.g. alpha 8-13Hz). Broadband power was defined as the area under the power spectrum between 0.5-48Hz (shaded area). The offset is the power at the lowest included frequency (0.5Hz). The slope of the power spectrum is indicated by the dashed line. In D, three hypothetical trajectories of patients' radiological volumes, magnetoencephalography (MEG) measurements and progression as determined by the tumor board*

are shown. Tumor volume was obtained from all available scans (indicated by blue dots). Example 1 represents a hypothetical patient with stable tumor volume. Example 2 represents a hypothetically radiologically progressive patient (i.e. increasing volume). Example 3 represent a hypothetical patient classified as having radiologically stable tumor volume, because the initial small increase in tumor volume became stable at the next time points (continuous line) or returned to a lower volume indicating potential pseudoprogression (dashed line). The time between MEG and progression as defined by the tumor board is marked with shaded blue and may deviate from radiological tumor growth as operationalized in our study.

Broadband and band-specific power have most often been linked to physiological, cognitive, behavioral, and disease states[14]. However, two new measures of brain activity have recently been introduced[14,15]: the offset of the power spectrum potentially may be more specifically related to neuronal spiking rates[15], while the slope of the power spectrum may reflect the balance between levels of excitation and inhibition of these neuronal populations[15]. We could thus hypothesize that all three measures of brain activity hold promise as markers of radiological tumor growth.

In a retrospective, cross-sectional setting, we evaluated postoperative global and peritumoral brain activity, operationalized as (1) broadband power, (2) offset and (3) slope of the power spectrum, and related these measures to tumor volume changes measured on routine MRI around the MEG. We hypothesized higher broadband power and offset and lower slope in patients showing increasing tumor volumes, as compared to patients with stable tumor volumes. Finally, we compared our findings for MEG to brain activity recorded with EEG (measured simultaneously with MEG), since MEG is costly and unavailable in most hospitals.

Methods

Subjects

Adult patients were selected from a previously collected cohort, included at the Amsterdam University Medical Centers (Amsterdam UMC, location VUmc) between 2007-2018[12,13,16]. Patients had undergone tumor resection and had histopathologically confirmed diffuse glioma World Health Organization

grade II, III or IV[17]. Patients were aged 18 years or older, and had no history of psychiatric or neurologic disease. Isocitrate dehydrogenase (IDH) mutation and 1p/19q codeletion status were obtained after 2016[17]. All patients underwent an MEG measurement after tumor resection. Tumor progression at the MEG timepoint was determined by the multidisciplinary tumor board, based on clinical and radiological characteristics. Time to tumor progression from the MEG was obtained in weeks. The MEG system was replaced in 2010, so we used the subsequent measurements as the main cohort, and the preceding recordings as a validation cohort (further information on this cohort is in the supplementary materials).

For comparison and normalization, we also included 36 healthy controls (HCs) from a previously described cohort[18,19], matched to patients at the group level for age, sex and educational level (Verhage system[20]).

Another cohort of postoperative diffuse glioma patients was prospectively included between 2019-2020 and underwent simultaneous MEG and EEG (MEEG; further information on this cohort is in the supplementary materials).

Radiological tumor growth

Routine MRIs up to one year after MEG were used for tumor segmentation. MRI was performed every 3 months for high-grade glioma (HGG), and every 6 months for low-grade glioma (LGG). For LGG, masks were created by segmenting the hyperintense area(s) on T2-weighted and/or FLAIR images. For HGG, contrast enhancing areas on T1-weighted images were masked. Tumor masks were semi-automatically segmented (smart brush tool of iPlan v3.0; BrainLAB AG, Feldkrichen, Germany) under supervision of an experienced neuroradiologist [BM]. Total mask volume was calculated for each MRI.

We first assessed radiological tumor growth as two continuous measures, by subtracting tumor volume on the last MRI before MEG from the first MRI after MEG, and calculating both an absolute volume change and a percentage volume change. Secondly, we classified patients into two groups: stable tumor volume if the difference in volume was <1 ml and increasing tumor volume if the volume

increase was >5 ml. Tumor volume increases between 1-5 ml were classified as increasing tumor volume if the following MRI showed further tumor growth, otherwise they were classified as stable tumor volume (figure 1D).

MEG acquisition and analyses

In the main cohort, MEG data was obtained with a 306-channel whole-head system (Elekta Neuromag Oy, Helsinki, Finland) with a sample frequency of 1250 Hz, and an online anti-aliasing (410 Hz) and high-pass (0.1 Hz) filter. Patients were in supine position inside a magnetically shielded room (VacuumSchmelze GmbH, Hanau, Germany) and were instructed to keep their eyes closed and stay awake during the 5 minute recording.

Data was visually inspected and a maximum of 12 malfunctioning channels were excluded. Temporally extended Signal Space Separation in Maxfilter software (Elekta Neuromag Oy, version 2.2.15)[21,22] was applied to remove artefacts, followed by application of a single-pass finite impulse response filter between 0.5-48 Hz.

Patients' head positions were recorded with four or five head position coils, which were digitized together with scalp shape before the recording, using a 3D digitizer (Fastrak, Polhemus; Colchester, VT, USA). Anatomical MRI was used for co-registration with MEG using a surface matching approach. Time-series from 78 cortical regions according to the Automated Anatomical Labeling atlas were obtained using a scalar beamformer implementation on the sensor-level signals using centroids (figure 1A (left panel) and 1B[23,24]).

In order to assess representative peritumoral brain activity, ten locations were manually selected in the grey matter around the tumor and/or resection cavity. These locations were all within 3 cm distance of the rim of the tumor mask and were placed in areas without evident edema. After establishing these ten locations, their ten homologue contralateral areas were also selected for analysis (figure 1A right panel). Scalar beamforming was performed to extract peritumoral and homologue contralateral time-series.

Time-series were split into epochs of 13.1s and visually inspected. The first ten artifact-free epochs were selected for further analysis. To assess the robustness of results with different epoch selection, the main analyses were repeated on the ten epochs with the highest alpha peak (maximum power in the 4-13 Hz band). The presence of a clear alpha peak reduces the probability that the subject was drowsy, which may impact brain activity[25].

Global brain activity

Brain activity was assessed using (1) absolute broadband power, and (2) offset and (3) slope of the power spectrum. For each epoch and each brain region, the power spectrum was obtained (figure 1C), using Welch's method with a Hamming window, and subsequently averaged across all epochs per patient. Broadband power was then calculated as the area under the curve between 0.5-48 Hz and averaged across all regions to obtain a single value per patient.

The offset and the slope of the power spectra were calculated using the Fitting Oscillations & One Over F (FOOOF) toolbox (https://github.com/fooof-tools/fooof) implemented in Python[14]. The non-oscillatory part of individual power spectra were fitted with an exponential function L: $L = b - \log(k + F^{\chi})$, where b is the offset, χ is the slope, F represents a vector with the frequencies and k is the knee parameter to set the bending of the aperiodic signal to 0 (i.e. no bending). The offset and slope (figure 1C) were averaged across all regions to obtain a single value per patient.

Peritumoral brain activity

Broadband power, slope and offset were also calculated with time-series from the selected peritumoral areas. To account for intraindividual variations due to the different tumor locations, normalized peritumoral brain activity was calculated by taking the ratio between brain activity of the peritumoral areas and their homologues in the contralateral hemisphere (figure 1A right panel).

Statistical analysis

Differences in demographics between patients and HCs were assessed using a Students' t-test (age) and χ^2-tests (sex, education).

In order to test our main hypotheses, brain activity was correlated with tumor growth using Spearman's correlations, and compared between stable versus increasing volume groups with Mann-Whitney U-tests.

Within patients, peritumoral brain activity was compared to homologue contralateral brain activity using paired Wilcoxon signed-rank tests. Brain activity was also compared between tumor grades, molecular tumor subtypes and epilepsy status (present or not) using Kruskal-Wallis tests, and correlated with preoperative tumor volumes using Spearman's correlation.

We also investigated the relationship of global brain activity with time to progression after MEG using multivariate Cox proportional hazards models with age and tumor grade as covariates, to enable comparison with our previous studies[12,13]. To do so, we computed z-scores of global brain activity based on the means and SDs of HCs. Kaplan-Meier curves were created using median splits of brain activity. Patients without progression as determined by the tumor board were censored after last contact with their treating neuro-oncologist.

Statistical analyses were performed using Python 3.6 (Python Software Foundation, www.python.org) and SPSS version 26 (IBM Corp., Armonk, NY, USA). *P*-values < 0.05 were considered significant, after correcting significance levels for the number of tests performed per analysis using the false discovery rate. In case of significant differences between groups, effect sizes were assessed using Cohen's D.

Results

Patient characteristics

In the main cohort, postoperative MEG was available in 50 patients. Four patients were excluded due to unavailable MRI follow-up, one patient was excluded because of low MEG quality. In total, 45 patients were included (table 1). Increasing radiological tumor volumes on the two scans surrounding

the MEG (see figure 1 above for a schematic representation of our analysis pipeline) were found in 18 patients (40%), of whom 7 (39%) had IDH-wildtype glioma, 8 (44%) had IDH-mutant 1p/19q non-codeleted glioma, 2 (11%) had IDH-mutant 1p/19q codeleted glioma, and 1 (6%) had an unknown molecular subtype.

Table 1. Patient characteristics

	Main cohort (n=45)
Age, mean ± SD	44.1 ± 14.0
Male, n (%)	32 (71%)
WHO Grade, n (%)	
II	26 (58%)
III	8 (18%)
IV	11 (24%)
Molecular subtype, n (%)	
IDH-mutant, 1p/19q codeleted	8 (18%)
IDH-mutant, non-codeleted	18 (40%)
IDH-wildtype	11 (24%)
Unknown	*8 (18%)*
Epilepsy present, n (%)	38 (84%)
Preoperative tumor volume (cm^3), mean ± SD	41.8 ± 32.3
Days between craniotomy and MEG, median (Q1-Q3)	312 (121-558)
Radiological follow-up around MEG	
Days between MRI and subsequent MEG, median (Q1-Q3)	85 (24-113)
Days between MEG and subsequent MRI, median (Q1-Q3)	50 (0-159)
Lateralization of tumor, n (%)	23 (51%)
Right	22 (49%)
Left	
Treatment during MEG	-
Radiotherapy	3 (7%)
Chemotherapy	
Change in radiological tumor volume	
Increasing tumor volume	18 (40%)
Stable tumor volume	27 (60%)

** No MRIs available after MEG. SD = standard deviation, Q1-Q3 = 1st quartile-3rd quartile.*

Global brain activity

For all three measures of brain activity, global brain activity did not correlate with tumor volume changes in ml or percentage (figure 2, supplementary table 1). There were also no differences in brain activity between patients with stable versus increasing tumor volumes (figure 3, supplementary table 2). However, global broadband power, offset and slope were significantly higher in both patient groups compared to healthy controls after correction for multiple comparisons (figure 3, supplementary table 2).

Figure 2. Correlations between tumor volume changes and global brain activity

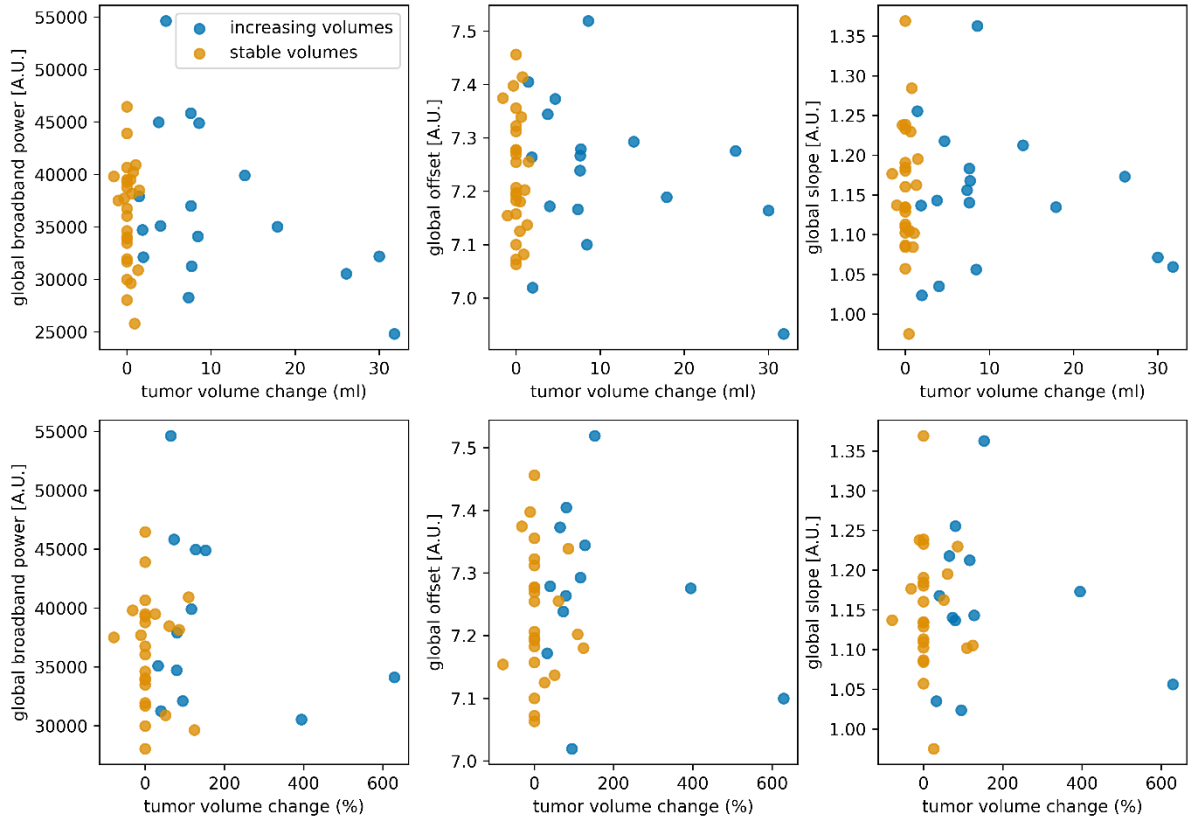

Legend. *No correlations were found between brain activity and tumor volume change expressed in ml (upper panels) or percent tumor volume change (lower panels). In eight patients, it was not possible to compute percent change, because the initial tumor volume was 0 ml. [A.U.] = arbitrary units.*

Figure 3. Global brain activity across groups

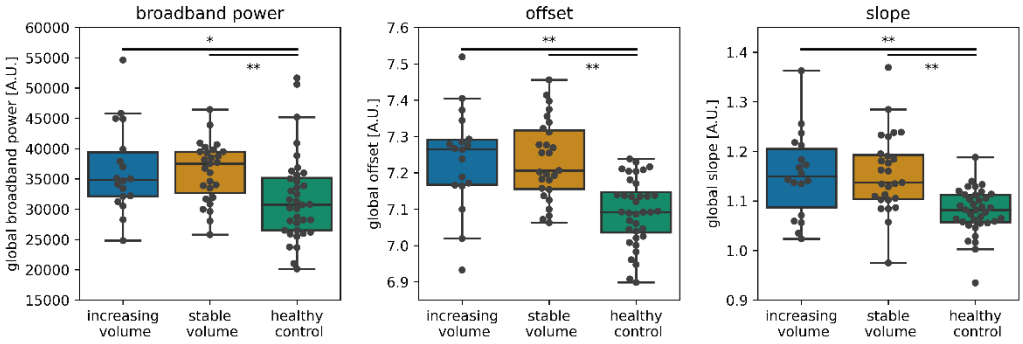

Legend. *Global brain activity was not different between patients with stable versus increasing tumor volumes. Both glioma groups showed higher global brain activity compared to healthy controls. Individual patients are represented by black dots. * P < 0.05, ** P < 0.01 after correction for multiple comparisons. [A.U.] = arbitrary units.*

Alternative epoch selection resulted in identical non-significant results regarding brain activity and tumor volume changes (supplementary materials), so further analyses were performed on the first ten epochs. The validation cohort corroborated all main results (supplementary materials).

Global broadband power, offset and slope were not related to tumor grade, molecular subtype or presence of epilepsy (supplementary figures 1-3). Preoperative tumor volume was not significantly related to global broadband power (rho(43) = 0.29, *P* = 0.05), however significant correlations with global offset and slope were found (rho(43) = 0.38, *P* = 0.01 and rho(43) = 0.37, *P* = 0.01, respectively, supplementary figure 4).

Peritumoral brain activity

Peritumoral brain activity (absolute and normalized for homologue contralateral brain activity) did not correlate with ml or percent tumor growth after correction for multiple comparisons (supplementary table 3), nor did it differ between patients with stable versus increasing radiological tumor volumes (supplementary table 4).

Significantly higher broadband power was found in the peritumoral areas as compared to their contralateral homologues (W = 108, $P < 0.01$, effect size D = 0.85; figure 4). Similar results were found for slope (W = 45, $P < 0.01$, D = 1.27) and offset (W = 13, $P < 0.01$, D = 1.23). These findings were replicated in the validation cohort (supplementary materials).

Figure 4. Brain activity of peritumoral and homologue contralateral areas

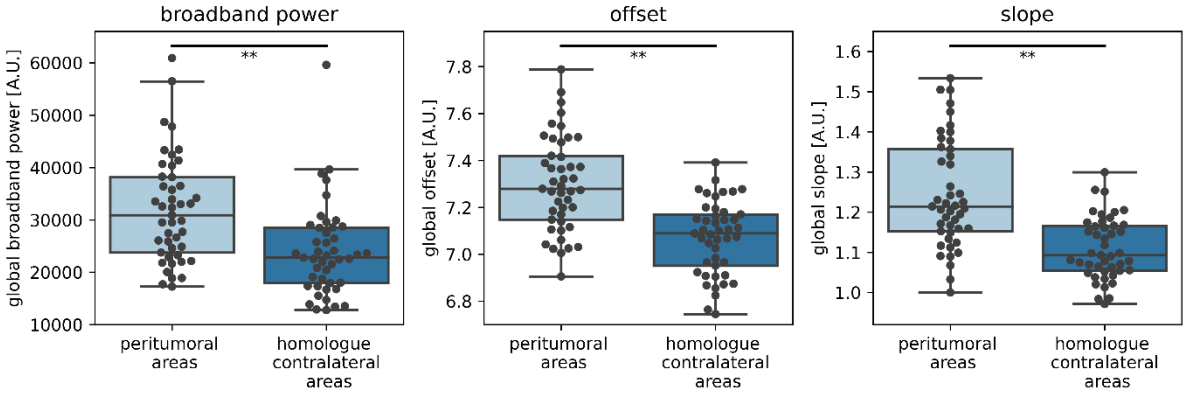

Legend. *Peritumoral brain activity was significantly higher compared to the homologue contralateral areas. ** P < 0.01 after correction for multiple comparisons. [A.U.] = arbitrary units.*

MEG versus EEG

In order to explore the potential of EEG of recapitulating the significant differences in MEG brain activity between the tumor and contralateral hemispheres, we repeated this analysis for MEG and EEG. Indeed, average brain activity of the tumor hemisphere was generally higher than contralateral brain activity for both modalities (supplementary figure 8). Note that due to the low spatial resolution of EEG, we did not establish peritumoral and contralateral homologues in this dataset.

Brain activity and time to progression

Progression as assessed by the tumor board was present in 26 patients (58%). Multivariate Cox proportional hazards analyses showed a hazard ratio of 2.48 (95% confidence interval (CI) 1.01-6.07, $P < 0.05$) for normalized broadband power in relation to time to progression, while slope and offset z-

scores were not associated with time to progression (supplementary table 5 and supplementary figure 5). In the validation cohort, there was no relation between brain activity and time to progression (broadband power: HR 1.00 (95% CI 1.00-1.00), *P* = 0.40, supplementary table 6).

Discussion

Contrary to our hypothesis, global and peritumoral brain activity did not correlate with tumor growth and did not distinguish between patients with stable versus increasing radiological tumor volumes in this heterogeneous cohort of diffuse glioma patients. However, brain activity was significantly higher in patients than in healthy controls. Moreover, patients' peritumoral brain activity was significantly higher than homologue contralateral areas. Finally, our preliminary findings suggest that EEG is able to recapitulate these increases in tumor-related MEG brain activity.

There are several possible explanations for the lack of association between brain activity and radiological tumor growth. Firstly, our patient cohort was heterogeneous in terms of tumor grade and molecular subtype, which may have obscured more subtle differences in brain activity relating to radiological tumor growth, particularly since histopathological subgroup differences in brain activity have been reported[26,27]. Patients were also in different phases of the disease and their treatment. It is unclear what the potentially confounding effects of chemotherapy and/or radiotherapy are on brain activity measurements with MEG and EEG.

Secondly, most of our patients had epilepsy and used anti-epileptic drugs (AEDs), but the relationship between activity-dependent tumor growth and epilepsy is unknown. In light of the bidirectional relationship between neuronal activity and glioma growth, one could hypothesize that suppressing neuronal activity with AEDs might reduce tumor growth[7,8,12,28]. Indeed, higher seizure frequency is related to worse prognosis[29]. Epidemiological studies have revealed contrasting relationships between AED use and (progression-free) survival: some report longer survival in patients on AEDs[30-34], others do not[35,36]. In this relatively small and heterogeneous sample, we did not find significant differences in brain activity between patients with or without epilepsy.

Thirdly, determining tumor volumes on MRI and subsequently classifying volume changes as stable or increasing is challenging and might be unreliable depending on imaging techniques used, although MRI currently remains the best marker for progression. In this retrospective study, inclusion of older data meant that additional and potentially informative MRI sequences, e.g. perfusion imaging, were not available in all patients. Therefore, subtle tumor growth might have gone unnoticed, while areas may also have been classified incorrectly as tumor due to pseudoprogression[37,38], particularly in HGG where tumor volumes were only determined on T1-weighted images after contrast injection. We did mitigate incorrect classifications as much as possible by evaluating all available scans, also those acquired after MEG.

Finally, our indirect measure of neuronal activity may be the culprit for a lack of effect: the animal studies reporting a bidirectional interaction between neuronal activity and glioma growth directly measured neuronal activity[5]. Conversely, broadband power, offset and slope based on MEG are indirect proxies of neuronal activity[15,39]. At the same time, our findings of higher broadband power and offset in the peritumoral regions do corroborate previous clinical findings using electrocorticography in GBM patients[7]. It could therefore also be that cross-sectionally measured brain activity is not able to differentiate between radiological progression and stable disease. To definitively assess whether brain activity is useful as a marker of tumor progression, future prospective, longitudinal studies in more homogeneous glioma populations and with more extensive standardized MRI and clinical evaluations are necessary.

Such studies may benefit from our findings: broadband power and offset were higher in patients than controls, and were higher in the peritumoral areas and/or ipsilateral hemisphere as compared to the contralateral hemisphere, for both MEG and EEG. In contrast to our expectations, the slope was steeper in patients than in controls and was higher in peritumoral areas, which potentially indicates relatively lower excitation than inhibition[14,15]. More shallow slopes were expected in patients and particularly in the peritumoral areas, since glioma has glutamate-dependent neurogliomal synapses that may raise the excitation-inhibition balance[7]. However, knowledge on the excitation-inhibition

balance *in vivo* is particularly scarce. Taken together, these findings suggest that focusing on brain activity of the peritumoral areas (as compared to their contralateral homologue areas) may potentially increase sensitivity to tumor growth when longitudinally following patients. Furthermore, our results may indicate that larger patient cohorts could also be investigated with EEG instead of MEG. Finally, the spectral slope does not seem a promising measure of brain activity to assess glioma growth.

In conclusion, brain activity is higher in glioma patients as compared to controls, and is higher in the peritumoral areas compared to their contralateral homologues across cohorts and MEG/EEG modalities. However, brain activity does not relate to ongoing radiological glioma growth. Longitudinal studies in more homogeneous and larger cohorts may use these insights to further explore the relevance of non-invasively measured brain activity as a marker of tumor progression.

References

1 Thust, S. C. *et al.* Glioma imaging in Europe: A survey of 220 centres and recommendations for best clinical practice. *Eur Radiol* **28**, 3306-3317, doi:10.1007/s00330-018-5314-5 (2018).
2 Villanueva-Meyer, J. E., Mabray, M. C. & Cha, S. Current Clinical Brain Tumor Imaging. *Neurosurgery* **81**, 397-415, doi:10.1093/neuros/nyx103 (2017).
3 Brown, P. D. *et al.* Detrimental effects of tumor progression on cognitive function of patients with high-grade glioma. *J Clin Oncol* **24**, 5427-5433, doi:10.1200/JCO.2006.08.5605 (2006).
4 Meyers, C. A. & Hess, K. R. Multifaceted end points in brain tumor clinical trials: cognitive deterioration precedes MRI progression. *Neuro Oncol* **5**, 89-95, doi:10.1093/neuonc/5.2.89 (2003).
5 Venkatesh, H. S. *et al.* Neuronal Activity Promotes Glioma Growth through Neuroligin-3 Secretion. *Cell* **161**, 803-816, doi:10.1016/j.cell.2015.04.012 (2015).
6 Venkatesh, H. S. *et al.* Targeting neuronal activity-regulated neuroligin-3 dependency in high-grade glioma. *Nature* **549**, 533-537, doi:10.1038/nature24014 (2017).
7 Venkataramani, V. *et al.* Glutamatergic synaptic input to glioma cells drives brain tumour progression. *Nature* **573**, 532-538, doi:10.1038/s41586-019-1564-x (2019).
8 Venkatesh, H. S. *et al.* Electrical and synaptic integration of glioma into neural circuits. *Nature* **573**, 539-545, doi:10.1038/s41586-019-1563-y (2019).
9 Murakami, S. & Okada, Y. Contributions of principal neocortical neurons to magnetoencephalography and electroencephalography signals. *J Physiol* **575**, 925-936, doi:10.1113/jphysiol.2006.105379 (2006).
10 Barnes, G. R., Hillebrand, A., Fawcett, I. P. & Singh, K. D. Realistic spatial sampling for MEG beamformer images. *Hum Brain Mapp* **23**, 120-127, doi:10.1002/hbm.20047 (2004).
11 Troebinger, L., Lopez, J. D., Lutti, A., Bestmann, S. & Barnes, G. Discrimination of cortical laminae using MEG. *Neuroimage* **102 Pt 2**, 885-893, doi:10.1016/j.neuroimage.2014.07.015 (2014).
12 Belgers, V. *et al.* Postoperative oscillatory brain activity as an add-on prognostic marker in diffuse glioma. *J Neurooncol* **147**, 49-58, doi:10.1007/s11060-019-03386-7 (2020).

13 Derks, J. *et al.* Oscillatory brain activity associates with neuroligin-3 expression and predicts progression free survival in patients with diffuse glioma. *J Neurooncol*, doi:10.1007/s11060-018-2967-5 (2018).

14 Donoghue, T. *et al.* Parameterizing neural power spectra into periodic and aperiodic components. *Nature Neuroscience* **23**, 1655-1665 (2020).

15 Gao, R., Peterson, E. J. & Voytek, B. Inferring synaptic excitation/inhibition balance from field potentials. *Neuroimage* **158**, 70-78, doi:10.1016/j.neuroimage.2017.06.078 (2017).

16 Derks, J. *et al.* Understanding cognitive functioning in glioma patients: The relevance of IDH-mutation status and functional connectivity. *Brain Behav* **9**, e01204, doi:10.1002/brb3.1204 (2019).

17 Louis, D. N. *et al.* The 2016 World Health Organization Classification of Tumors of the Central Nervous System: a summary. *Acta Neuropathol* **131**, 803-820, doi:10.1007/s00401-016-1545-1 (2016).

18 Tewarie, P. *et al.* Structural degree predicts functional network connectivity: a multimodal resting-state fMRI and MEG study. *Neuroimage* **97**, 296-307, doi:10.1016/j.neuroimage.2014.04.038 (2014).

19 Tewarie, P. *et al.* Functional brain networks: linking thalamic atrophy to clinical disability in multiple sclerosis, a multimodal fMRI and MEG study. *Hum Brain Mapp* **36**, 603-618, doi:10.1002/hbm.22650 (2015).

20 Verhage, F. *Intelligentie en leeftijd: Onderzoek bij Nederlanders van twaalf tot zevenenzeventig jaar.* , (1964).

21 Taulu, S. & Hari, R. Removal of magnetoencephalographic artifacts with temporal signal-space separation: demonstration with single-trial auditory-evoked responses. *Hum Brain Mapp* **30**, 1524-1534, doi:10.1002/hbm.20627 (2009).

22 Taulu, S. & Simola, J. Spatiotemporal signal space separation method for rejecting nearby interference in MEG measurements. *Phys Med Biol* **51**, 1759-1768, doi:10.1088/0031-9155/51/7/008 (2006).

23 Hillebrand, A., Barnes, G. R., Bosboom, J. L., Berendse, H. W. & Stam, C. J. Frequency-dependent functional connectivity within resting-state networks: an atlas-based MEG beamformer solution. *Neuroimage* **59**, 3909-3921, doi:10.1016/j.neuroimage.2011.11.005 (2012).

24 Hillebrand, A. *et al.* Direction of information flow in large-scale resting-state networks is frequency-dependent. *Proceedings of the National Academy of Science USA* **113**, 3867-3872 (2016).

25 van Diessen, E. *et al.* Opportunities and methodological challenges in EEG and MEG resting state functional brain network research. *Clin Neurophysiol* **126**, 1468-1481, doi:10.1016/j.clinph.2014.11.018 (2015).

26 de Jongh, A. *et al.* The influence of brain tumor treatment on pathological delta activity in MEG. *Neuroimage* **20**, 2291-2301, doi:10.1016/j.neuroimage.2003.07.030 (2003).

27 Wilson, T. W., Heinrichs-Graham, E. & Aizenberg, M. R. Potential role for magnetoencephalography in distinguishing low- and high-grade gliomas: a preliminary study with histopathological confirmation. *Neuro Oncol* **14**, 624-630, doi:10.1093/neuonc/nos064 (2012).

28 Venkataramani, V., Tanev, D. I., Kuner, T., Wick, W. & Winkler, F. Synaptic Input to Brain Tumors: Clinical Implications. *Neuro Oncol*, doi:10.1093/neuonc/noaa158 (2020).

29 Vecht, C. J., Kerkhof, M. & Duran-Pena, A. Seizure prognosis in brain tumors: new insights and evidence-based management. *Oncologist* **19**, 751-759, doi:10.1634/theoncologist.2014-0060 (2014).

30 Lu, V. M., Jue, T. R., Phan, K. & McDonald, K. L. Quantifying the prognostic significance in glioblastoma of seizure history at initial presentation: A systematic review and meta-analysis. *Clin Neurol Neurosurg* **164**, 75-80, doi:10.1016/j.clineuro.2017.11.015 (2018).

31 Toledo, M. *et al.* Epileptic features and survival in glioblastomas presenting with seizures. *Epilepsy Res* **130**, 1-6, doi:10.1016/j.eplepsyres.2016.12.013 (2017).

32 Pallud, J. & McKhann, G. M. Diffuse Low-Grade Glioma-Related Epilepsy. *Neurosurg Clin N Am* **30**, 43-54, doi:10.1016/j.nec.2018.09.001 (2019).

33 Roh, T. H. *et al.* Association between survival and levetiracetam use in glioblastoma patients treated with temozolomide chemoradiotherapy. *Sci Rep* **10**, 10783, doi:10.1038/s41598-020-67697-w (2020).

34 Brodie, S. A. & Brandes, J. C. Could valproic acid be an effective anticancer agent? The evidence so far. *Expert Rev Anticancer Ther* **14**, 1097-1100, doi:10.1586/14737140.2014.940329 (2014).

35 van Breemen, M. S. *et al.* Efficacy of anti-epileptic drugs in patients with gliomas and seizures. *J Neurol* **256**, 1519-1526, doi:10.1007/s00415-009-5156-9 (2009).

36 Berendsen, S. *et al.* Prognostic relevance of epilepsy at presentation in glioblastoma patients. *Neuro Oncol* **18**, 700-706, doi:10.1093/neuonc/nov238 (2016).

37 Thust, S. C., van den Bent, M. J. & Smits, M. Pseudoprogression of brain tumors. *J Magn Reson Imaging* **48**, 571-589, doi:10.1002/jmri.26171 (2018).

38 van West, S. E. *et al.* Incidence of pseudoprogression in low-grade gliomas treated with radiotherapy. *Neuro Oncol* **19**, 719-725, doi:10.1093/neuonc/now194 (2017).

39 Manning, J. R., Jacobs, J., Fried, I. & Kahana, M. J. Broadband shifts in local field potential power spectra are correlated with single-neuron spiking in humans. *J Neurosci* **29**, 13613-13620, doi:10.1523/JNEUROSCI.2041-09.2009 (2009).